International Journal of Sciences and Techniques of Automatic control & computer engineering
IJ-STA, Volume 4, N° 1, July 2010, pp. 1188–1197.

Electric field attenuation of an Ultra Wide Band wave (UWB) during propagation in the human body

Moez Ketata, Mohamed Dhieb, Mondher Chaoui,
Mongi Lahiani and Hamadi Ghariani

Laboratory of electronics and information technologies (LETI) ENIS, BP W, 3038 SFAX, TUNISIA.
E-mail: m.kketata@yahoo.fr

Abstract. *This work is part of the studies concerning the use of **U**ltra **W**ide **B**and (UWB) for conducting bio-medical sensing and monitoring of human vital signs, in which we study the Gaussian pulse propagation in the human body through the skin, muscles, chest and lung in order to hit the walls of the heart and come back to the radar antenna where the information is acquired. These layers will be modeled by their relative dielectric constant, their thickness and their electric conductivity. The aim of this study is to solve Maxwell's equation in these environments for calculating the attenuation of the wave in each layer. There are several methods to be used such as **F**inite **E**lement **M**ethod (**FEM**) and the **F**inite **D**ifferences **T**ime **D**omain (**FDTD**) method. In our work we choose the latter to simulate Maxwell's equations in order to see the wave during there propagation in different areas. The source is a simple Gaussian pulse plane and uniform which normally tackles the surface of the skin. The frequency is fixed at 4.1 GHz. These features simplify the solution of equations that to be a single dimension, where the electric amplitudes fields and magnetic induction fields are dependent on the z-axis propagation and they are directed successively by the x-axis and y-axis.*

Keywords. *FDTD, attenuation, UWB wave, human body tissue*.

1. Introduction

In the previous works, [1, 2, 3, 4] the estimate attenuation undergone by a Gaussian pulse in human body was made, but they give only a rough approximation to solve the Maxwell's equations. This analysis in full wave could give more reliable results. In our paper, we use a one-dimensional FDTD simulation to evaluate the performance propagation of a Gaussian pulse in human tissues.

This paper was recommended for publication in revised form by the editor Staff.
Edition: CPU of Tunis, Tunisia, ISSN: 1737-7749

The FDTD is a versatile modeling technique used to solve Maxwell's equations. It is obvious, so that users can easily understand how to use it and recognize what to expect from a given model. This method is a time-domain technique, when a broadband pulse (such as a Gaussian pulse) is used as the source. Thus the response of the system over a wide range of frequencies can be obtained with a single simulation. This is useful in applications where resonant frequencies are not exactly known, or when ever a broadband result is desired.

The FDTD lends itself to providing animated displays of the electromagnetic field movement through the model. This type of display is useful in understanding what is going on in the model, and to help ensure that the model is working correctly.
In accord, we can deduce the attenuation in biological tissue which differs by comparing the amplitude of the transmitted wave in any point of the layer to the incident that exists at the interface between any two layers.

2. Model of the human body

The source "antenna" is located at a distance of 15 cm from the air /skin interface because it is the maximum distance obtained in previous approximations where losses in air are negligible [1, 2, 3, 5]. Consequently, the resulting weakening of the simulation is due solely to spread through tissue. This device is shown in Figure1.

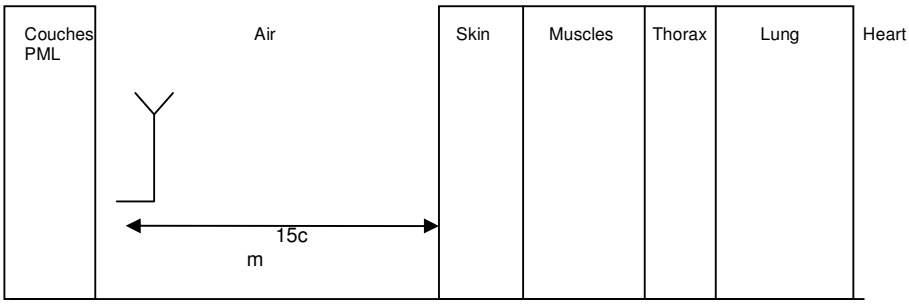

Fig 1. Simplified model of human textile composed of 4 layers of semi-infinite.

i.e.: The PML will be developed to be on.

The studied part of the human body's tissue is composed of four semi-infinite layers. These have been characterized by their complex relative dielectric constant [6], their thickness and their electric conductivity [5,7,8] as given in Table 1

Table1. Thickness, Conductivity and dielectric constant of the various layers of human tissue.

Type of the Standard layer	Thickness [cm]	Cconductivity ∂ [S/m]	dielectric constant ε_r at 4GHz
Skin	0.96	0.25	5.5
Muscles	1.35	3.50	50.5
thorax	1.16	3.00	35.0
Lung	0.578	1.50	20.0

3. Model of the UWB source

The pulses can be created in different ways including the Hermit impulsion which is based on polynomial function and the monocycles impulsion which is the first derivative of Gaussian pulse [9], the purpose of this work is to adopt the Gaussian pulse [10]given by equation 1 witch is displayed in the following forms (fig.2).

$$f(t) = k_p e^{-\left(\frac{t-t_0}{a}\right)^2}$$
$$a = \frac{1}{\pi\sqrt{2} f_c} \cong 50ps, \quad f_c = 4.1GHz \tag{1}$$

where: - f_c: is the frequency of work.
- t_0: is the delay time from the origin of the Gaussian impulse.
- a: is the width's time of the Gaussian impulse

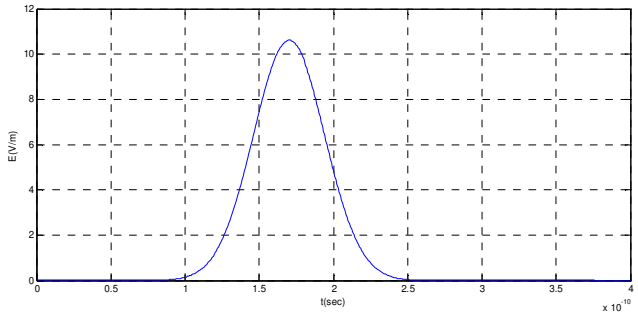

Fig. 2. The Gaussian pulse

The spectrum of this Gaussian is given by Fourier Transforming (eq.2)

$$Tf\left[f(t)\right] = \tilde{f}(\omega) = \frac{1}{\sqrt{2\pi}} \int_{-\infty}^{+\infty} f(t) e^{-iwt} dt$$
$$f(\omega) = \frac{1}{2} k_p \pi \sqrt{\pi} a^3 \pi e^{-2\pi\omega} \tag{2}$$

where ω :is the pulsation of UWB wave.
The spectrum of this Gaussian is shown in figure 3.

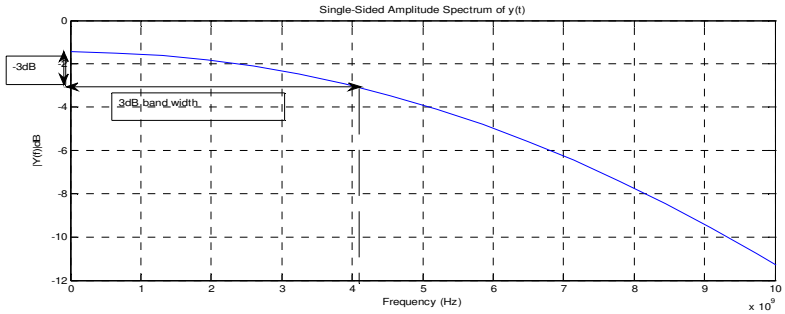

Fig 3. Spectrum of this Gaussian pulse given by Fourier transforming

From this curve, we can deduce the pulse frequency which is the abscissa of the ordered-3dB maximum.

4. One-dimensional FDTD Method:

The FDTD is a numerical method for electromagnetic modeling [11] using a spatial and temporal discretization of Maxwell's equations. This work uses a one dimensional FDTD simulation to asses the propagation performance in tissues of the Gaussian impulsion.

4-1. Maxwell's equations:

The electro-magnetic equations of Maxwell may be written as:

$$\begin{aligned} &- \quad \frac{\partial D}{\partial t} = \nabla * H \\ &- \quad \frac{\partial H}{\partial t} = -\frac{1}{\mu_0} \nabla * E \\ &- \quad D(\omega) = \varepsilon_0 \varepsilon_r(\omega) E(\omega) \end{aligned} \tag{3}$$

where
D: Electric flux density vector [C/m^2]
E: Electric field intensity vector [V/m]
H: Magnetic field intensity vector [A/m]
μ_0: Free space permeability = $4\pi.10^{-7}$ [H/m]

In particular: $D = D(\omega) = \varepsilon_0 \varepsilon_r(\omega) E(\omega)$

Where ε_0: Free space permittivity = $8.854.10^{-12}$ [F/m]
$\varepsilon_r(\omega)$ *:* complex relative dielectric constant dependant of frequency.

The electric field directed along the x-axis "and the magnetic induction along the y-axis

$$\begin{aligned} - \quad & \vec{E} = E(z)\vec{x}; \quad \vec{H} = H(z)\vec{y} \\ - \quad & \frac{\partial \tilde{D}}{\partial t} = -\frac{1}{\sqrt{\varepsilon_0 \mu_0}} \frac{\partial H}{\partial z} \\ - \quad & \frac{\partial H}{\partial t} = -\frac{1}{\sqrt{\varepsilon_0 \mu_0}} \frac{\partial \tilde{E}}{\partial z} \end{aligned} \tag{4}$$

4-2. One dimensional FDTD Method

Electric field is evaluated in each time step and each cell space based components that precede it. This method works in time domain and allows direct visualization of electric and magnetic fields. The FDTD is independent of the geometry of the model system. In fact, we can cover a wide spectrum of frequencies with a single simulation. In addition it is possible to model the behaviour of dispersion environments, and to highlight a non-reciprocal propagation. Thus, we can define a spatial-temporal grid as each time interval of the propagation medium is divided into intervals of space so that the fields that describe the propagation of UWB waves are almost constant in each cell space [11] and [12]. According to the above Maxwell's equations become:

$$\begin{aligned} \frac{\tilde{D}_x^{n+\frac{1}{2}}(k) - \tilde{D}_x^{n-\frac{1}{2}}(k)}{\Delta t} &= -\frac{1}{\sqrt{\mu_0 \varepsilon_0}} \frac{H_y^n\left(k+\frac{1}{2}\right) - H_y^n\left(k-\frac{1}{2}\right)}{\Delta z} \\ \frac{H_y^{n+1}\left(k+\frac{1}{2}\right) - H_y^n\left(k+\frac{1}{2}\right)}{\Delta t} &= -\frac{1}{\sqrt{\mu_0 \varepsilon_0}} \frac{\tilde{E}_x^{n+\frac{1}{2}}(k+1) - \tilde{E}_x^{n+\frac{1}{2}}(k)}{\Delta z} \end{aligned} \tag{5}$$

This yield:

$$\begin{aligned} \tilde{D}_x^{n+\frac{1}{2}}(k) &= \tilde{D}_x^{n-\frac{1}{2}}(k) - \frac{\Delta t}{\Delta z \sqrt{\mu_0 \varepsilon_0}} \left(H_y^n\left(k+\frac{1}{2}\right) - H_y^n\left(k-\frac{1}{2}\right) \right) \\ H_y^{n+1}\left(k+\frac{1}{2}\right) &= H_y^n\left(k+\frac{1}{2}\right) - \frac{\Delta t}{\Delta z \sqrt{\mu_0 \varepsilon_0}} \left(\tilde{E}_x^{n+\frac{1}{2}}(k+1) - \tilde{E}_x^{n+\frac{1}{2}}(k) \right) \end{aligned} \tag{6}$$

4-3. Determination of cell size

To determine Δt, we must take into account that the electromagnetic wave which is propagating in free space can not go faster than the speed of light. So if it propagates a distance of a cell needs a time minimum of $\Delta t = \Delta z / C_0$. Where C_0 is just the special case of a more general term known as the "current status", which establishes that for n dimensions [13]:

For n-dimensional system:

$$\Delta t \geq \frac{\Delta z}{\sqrt{n}\,C_0} \tag{7}$$

if n = 2

$$\Delta t \approx \frac{\Delta z}{\sqrt{2}C_0} \approx \frac{\Delta z}{2C_0} \tag{8}$$

The Experience proves that a good rule of thumb for the size of cells happens to be:

$$\begin{aligned} \Delta z &= \frac{\lambda_{\min}}{10} \\ \lambda_{\min} &= \frac{V_{\min}}{f_{\max}} = \frac{C_0}{f_{\max}\sqrt{\varepsilon_{r_{\max}}}} \end{aligned} \tag{9}$$

For human tissue, it was $\varepsilon_{r_{\max}}$ =35 and f_{max}=10 GHz by the FFC [10] thus

$\lambda_{\min} = 4.78 * 10^{-3}\, m = 4.78 mm$; $\Delta z \approx 0.45 mm$

5. Definition of Perfectly Matched Layers "PML"

We introduce **P**erfectly **M**atched **L**ayers (PML) layers on both sides of the layers of interest to prevent the wave reflection at the borders. In fact, it will be absorbed and strongly attenuated in these layers. The propagation in these layers is characterized by the following Maxwell equations: [5]

$$\begin{aligned} \tilde{D}_x^{n+\frac{1}{2}}(k) &= g_{k,3}(k)\tilde{D}_x^{n-\frac{1}{2}}(k) - \frac{\Delta t}{\Delta z\sqrt{\mu_0\varepsilon_0}}\, g_{k,2}(k)\left(H_y^n\left(k+\frac{1}{2}\right) - H_y^n\left(k-\frac{1}{2}\right)\right) \\ H_y^{n+1}\left(k+\frac{1}{2}\right) &= f_{k,3}\left(k+\frac{1}{2}\right)H_y^n\left(k+\frac{1}{2}\right) - \frac{\Delta t}{\Delta z\sqrt{\mu_0\varepsilon_0}}\, f_{k,2}\left(k+\frac{1}{2}\right)\left(\tilde{E}_x^{n+\frac{1}{2}}(k+1) - \tilde{E}_x^{n+\frac{1}{2}}(k)\right) \end{aligned} \tag{10}$$

with:

$$\begin{aligned} f_{k,2}\left(k+\frac{1}{2}\right) &= \frac{1}{1+x_n\left(k+\frac{1}{2}\right)};\; f_{k,3}\left(k+\frac{1}{2}\right) = \frac{1-x_n\left(k+\frac{1}{2}\right)}{1+x_n\left(k+\frac{1}{2}\right)} \\ g_{k,2}(k) &= \frac{1}{1+x_n(k)};\; g_{k,3}(k) = \frac{1-x_n(k)}{1+x_n(k+)} \end{aligned} \tag{11}$$

where x_n is an empirical formula that carries in the following form:

$$x_n(k) = PML\_ATT\_FACTOR * \left(\frac{k}{PML\_length}\right)^3$$
$$PML\_ATT\_FACTOR = 0.8;\ 0.3;\ 0.1 \qquad (12)$$
$$PML\_length = 40$$

6. Simulation results

6-1. Effect of the Interference phenomenon

The results of the simulation for two nearing times (at t_1=1398[ps] and t_2=1420[ps]) are show in figure 4.

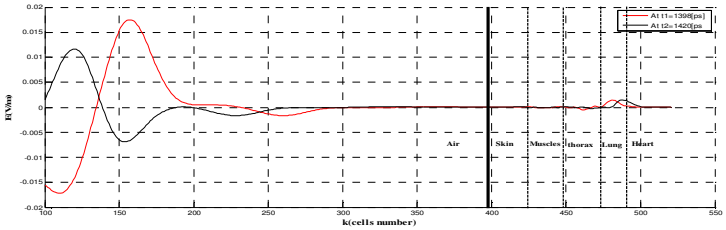

Fig. 4. Simulation of Gaussian monocycle impinging multiple layers of lossless tissues.

We notice that the distribution field E in all space was obtained, has a small difference is due to the interaction of the reflected part of the wave that already penetrated the heart wall which briefly delays the arrival of the maximum from the theoretical value.

6-1. attenuation in fields' amplitude

We can deduce that the attenuation in biological tissue differs by comparing the amplitude of the wave transmitted from any point of the layer to the incident that is in the interface between any two layers as shown in figure 5.

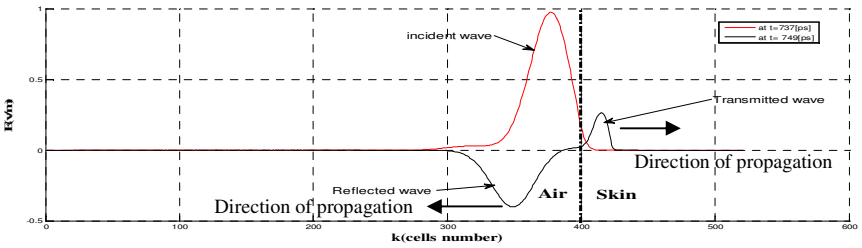

Fig. 5.Incident, Transmitted and Reflected wave at the interface Air-Skin as function as cells number

At 737[ps], the wave has just hit the air-skin interface: it's the incident wave after a certain time (at 749[ps]) the wave is divided into two parts:

- One that will complete its spread in the skin: it's the transmitted wave.
- The other goes back to the source antenna: it's the reflected wave.

Attenuation is defined as the quotient in dB between the maximum of both electric fields' amplitudes in each part of layers and the maximum amplitude of incident fields that exists on the interface (equation 13).

$$Att = 10 * \log_{10}\left(\left|\frac{E_{\max}(n,k)}{E_{\text{incident}}}\right|^2\right) \tag{13}$$

with $E_{max}(n_0, k)$ is the maximum amplitude of the E fields at $t=n_0*\Delta t$ and $z=k*\Delta z$. $E_{incident}$ is the maximum amplitude of the pulse incident when the wave hits the interface between two layers. The results of simulation are presented in Figure 6.

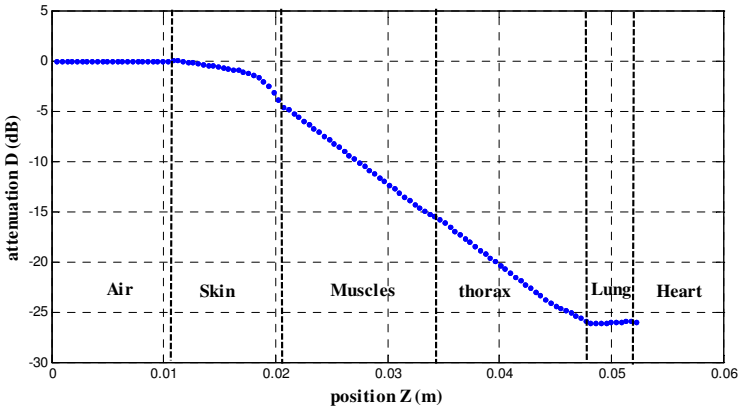

Fig. 6. Attenuation: Att (dB) of the amplitude of the electric field in each layer as a function of position Z(m)

This figure displays the attenuation of pulse intensity traveling from the transmitting antenna to the walls of the heart boundary. The decrease of the curve accounts for linear attenuation in the tissue (imaginary parts of reflection coefficient reflections and multiple reflections are ignored). The table.2 summarizes the values of attenuation in each layer:

Table 2. Values of the amplitude and attenuation in each layer

interface layers	attenuation of the amplitude of the E field compared to the amplitude of source (dB)
Air-skin	0
Skin-muscle	-5
Muscle-cartilage	-15
Cartilage-lung	-22
Lung-heart	-26

The wave attack border's heart at 1399 [ps] with an amplitude of $1.46*10^{-4}$ [V/m], the incident amplitude at the interface chest-lung is $2.8*10^{-3}$[V/m], bring about an attenuation of 26 dB. Comparing to other models which exist in biographies as Bilich in [2], the attenuation is nearing -30dB, therefore, we can be said that this model give a good results.

In our Calculate, we didn't take into consideration the reports echo, because the reflected wave has undergone several deformations due to the phenomenon of interference that disrupts the calculated attenuation.

7. Conclusions

A very close similarity is noticed between attenuation of the wave in the human body and that found in the bibliography. The current model of the human body is useful for simulating the spread of UWB wave by the FDTD method, especially in the transmitted parts of wave.

The FDTD simulations are the first step in understanding the propagation of UWB waves. We could take other approaches to describe the model of the human body such as Cole-for-Cole that describes dielectric constant. In this model the parameter becomes complex, this change will completely modify the simulation program; we can start the program from the Z transformer, which can be a future work. We can also extend the modeling in 2D or 3D and study the scattering characteristics of the heart, that was considered here as a semi-infinite media which is not exactly the case because its dimensions are not much higher than λ.

The severe attenuation of the wave in the body is not nullifying the benefits of using UWB pulses in opposition to other approach such as the use of single frequency.

References

1. Bilich, C. G.:Feasibility of Dual UWB Heart Rate Sensing and Communications Under FCC Power Restrictions. Third International Conference on Wireless and Mobile Communications, ICWMC (2007)
2. Bilich, C. G.: Bio-Medical Sensing Using Ultra Wideband Communications and Radar Technology: A Feasibility. Study. First International Conference on Pervasive Computing Technologies for Health Care 2006, IEEE, create-net, icst, Innsbruck, Austria (2009).
3. Bilich, C. G.: Bio-Medical Sensing Using Ultra Wideband Communications and Radar Technology. 20th Cycle of the Program in Information and Communications Technologies; Department of Information and Telecommunications Technology; University of Trento; Italy; January 2009.
4. Bilich, C. G.: UWB Radars for Bio-Medical Sensing: Attenuation Model for Wave Propagation in the Body at 4GHz. Technical Report DIT-06-051, Informatica e Telecomunicazioni, University of Trento, Aug.
5. S K, uha, M R,Khan and S N Tandon. : Electrical field distribution in the human body. IOP electronic journals Print publication: Issue 5 (September 1973)
6. Klein, L.Swift, C.:An improved model for the dielectric constant of sea water at microwave frequencies. Oceanic Engineering, IEEE Journal of , vol.2, no.1, pp. 104-111, Jan 1977
7. Staderini, E.M.: UWB Radars in Medicine. Aerospace and Electronic Systems Magazine, IEEE, Volume 17 (2002) 13–18.
8. S.Gabriel, R.W.Lau and C.Gabriel.:The dielectric properties of biological tissues: II. Measurements in the frequency range 10 Hz to 20 GHz. Phys. Med. Biol. 41 (1996), 2251-2269.
9. PulsON® Technology Overview, Huntsville, AL, USA (2001).
10. Reed J.H. Books online: An Introduction to Ultra Wideband Communication Systems: ISBN 0131481037
11. K. S,Yee. : Numerical Solution of Initial Boundary Value Problems Involving Maxwell's Equations in Isotropic Media, IEEE Trans. Antennas Propag., (1966) 302–307
12. Takefumi Namiki.: A New FDTD Algorithm Based on Alternating-Direction Implicit Method. IEE transactions on microwave theory and techniques, vol. 47, no. 10, october 1999.
13. Bilich, C.:A Simple FDTD Model to Asses the Feasibility of Heart Beat Detection using commercial UWB communication devices. Technical Report # DIT-07-033 38050 Povo – Trento (Italy), Via Sommarive 14.